LA-10657-MS

c. 3

*Bistatic Phase Sounding
in the Ionosphere
above the Minor Scale Explosion*

Los Alamos

Los Alamos National Laboratory
Los Alamos, New Mexico 87545
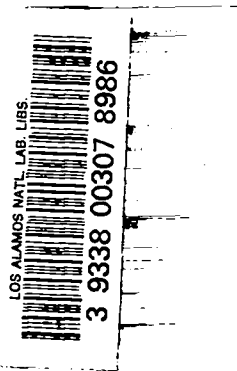
Bistatic Phase Sounding
in the Ionosphere
above the Minor Scale Explosion

Joseph Fitzgerald*

*Arnparo Corporation. P.O. Box 36780, Albuquerque, NM 87176.

Los Alamos Los Alamos National Laboratory
Los Alamos, New Mexico 87545

BISTATIC PHASE SOUNDING IN THE IONOSPHERE ABOVE THE MINOR SCALE EXPLOSION

by

Joseph Fitzgerald

ABSTRACT

A 4.8-kT chemical explosion named Minor Scale was detonated at the White Sands Missile Range on June 26, 1985. Following the detonation, three bistatic HF phase sounders observed disturbances in the ionosphere directly over the explosion. The path from transmitters to receivers, which were 283 km apart, had a midpoint 7 km northeast of ground zero. We describe the experiment and present time histories of the power spectra of the three transmissions. Between 300 and 360 s after the explosion, all three links showed changes in spectra. The lowest frequency shifted by -1 Hz, indicating the passage of the acoustic wave from the explosion through the total reflection height in the E-layer at about 95 km. We model the Doppler shift and absorption change to be expected for this disturbance assuming the acoustic wave had an N-wave profile with a maximum amplitude of 15%. The spectra of the lowest frequency also show temporary peaks at negative Doppler that indicate partial reflection modes from upper and lower edges of the N-wave. We calculate the Doppler shift and reflection coefficients for these partial reflection modes. During the same time period, the spectra of the two higher frequency transmissions also showed temporary peaks at negative Doppler that rapidly changed their frequency offset. From 380 to 480 s after the explosion, broad peaks at negative Doppler shift appeared in the spectra of the two higher frequencies. These peaks could be caused by reflection in the F-region induced by a temporary increase in the critical frequency by the passage of the acoustic wave from the explosion. We calculate the Doppler shift to be observed from such a mode.

1

I. INTRODUCTION

In June 1985 the U.S. Defense Nuclear Agency detonated 4.8 kt of conventional explosive, code-named Minor Scale, on the ground at White Sands Missile Range, New Mexico. When the acoustic wave from such an explosion reaches the ionosphere, it induces large changes in electron density; these changes, in turn, affect radio waves reflected from the ionosphere. The Los Alamos National Laboratory sponsored a number of ionospheric sounding experiments in conjunction with Minor Scale. We report here on one of these experiments: the measurement of phase changes in HF transmissions between geographically separated transmitters and receivers (bistatic phase sounding) over a path that reflected in the ionosphere almost directly above the explosion. Measurements of phase path change versus time characterize the ionospheric disturbance in terms of Doppler shifts and spectral changes. The aim of the experiment was to observe the ionospheric disturbance in both the E- and F-layers using three sounding frequencies.

Because of the relatively great amplitude of the acoustic wave, a Doppler shift in a transmission reflected in the E-layer was expected. Compared with the F-region, the E-layer has a steep electron density gradient, so the phase path change induced by an acoustic disturbance is smaller than that induced in the F-region. Therefore the Doppler shifts may be unobservable unless an unusually large amplitude wave traverses the E-layer. The Minor Scale explosion provided a source for such a wave. We expected that the acoustic wave would have an N-wave profile at the E-layer since pulses like those produced by explosions usually evolve into an N-wave shape. An N-wave profile is just one cycle of a sawtooth; that is, the perturbation $p(x)$ at distance x is given by

$$p(x) = \begin{cases} p_0 x/x_0 & |x| < x_0 \\ \\ 0 & \text{otherwise} \end{cases} , \qquad (1)$$

where p_0 is the amplitude and $2x_0$ is the length of the perturbation. We hoped that the duration and time development of the Doppler shift would enable us to estimate the amplitude and length of the N-wave profile.

The leading and trailing edges of the N-wave induce steep gradients in electron density as the acoustic wave traverses the E-layer. Although the transition region at $|x_0|$ in Eq. (1) will not be infinitesimal as indicated, we expected it to have a width comparable to or smaller than the wavelength of the HF radio transmission used to probe the ionosphere. We therefore hoped that partial reflections of the HF wave could be observed during the time that the N-wave traverses the E-layer below the height of total reflection and could be distinguished from the normal transmission by a Doppler shift caused by the upward motion of the partially reflecting layer. We expected that the partial reflection would eventually merge with the total reflection from the E-layer. It was also conjectured that partial reflections from both the leading and the trailing edges of the N-wave were possible.

As the acoustic wave traveled up into the F-region, we expected to see characteristic Doppler shifts in F-mode transmissions. (We adopt the convention that E, E_s, and F will indicate single-hop reflection from the corresponding layers.) From these Doppler shifts we hoped to determine the amplitude and profile of the acoustic wave at the 150- to 250-km altitude range and thus the time development of the wave between the E-layer and the F-region. Partial reflections were not expected at the F-region because the transition width of the N-wave increases with altitude and eventually becomes greater than the wavelength of the HF transmission.

We also expected that the E-layer would remain disturbed or turbulent after the passage of the N-wave. This turbulence would be observed as random, small-amplitude Doppler shifts in E-mode transmissions and also in changes in signal strength of these transmissions. Such effects would be observed as a broadening of the spectra and could persist for many minutes. It was also expected that sporadic E (E_s) would develop or change after the passage of the N-wave.

Besides the bistatic experiment described in this report, a number of other ionospheric sounding experiments attempted to determine the local (150-km-radius) disturbance caused by the Minor Scale explosion. Los Alamos operated a four-frequency vertical incidence phase sounder at about 7.5-km ground range from the explosion. Los Alamos also operated a 10-frequency HF radar and an 8-station bistatic network approximately 100 km to the west of the explosion (Jacobson et al., 1986). A French group performed ionospheric sounding experiments in conjunction with the explosion: a vertical incidence

3

sounder at about 35 km from ground zero and a bistatic network about 150 km east of the explosion.

Ionospheric disturbances following explosions have been observed during the last three decades. During the Buster-Jangle series of atmospheric nuclear explosions at the Nevada Test Site in 1951, an ionosonde at a ground range of 10 km was used to observe changes in group height caused by the acoustic wave (Kanellakos and Nelson, 1972). The explosions had yields that ranged from 5 to 30 kT. Temporary cusps appeared in the ionogram between 6 and 10 min after the explosions. These cusps were interpreted as caused by the leading and trailing edges of the acoustic wave, which induced temporary peaks in the electron density profile. The ionograms showed enhanced two-hop E-layer propagation between 5 and 6 min after the explosions, but these observations were not interpreted.

Vertical incidence phase sounders were used to monitor the ionospheric effects following the detonation of 500 tons of conventional explosive in 1964 (Barry et al., 1966). The sounders were 85 km from ground zero. Cyclical Doppler shifts began about 10 min after the explosion, and they corresponded to the passage of the acoustic wave through the total reflection height of 200 to 250 km. Barry et al. predicted a relative overpressure of 2.2% in the F-region; the observed phase path changes were approximately consistent with this prediction.

For the Mill Race explosion of 1981, which had a yield of 600 tons, a vertical incidence phase sounder was deployed by Los Alamos at a ground range of 5 km (Rickel and Simons, 1982). The ionospheric disturbance was observed at three frequencies corresponding to reflection heights between 150 and 250 km. No data corresponding to E-layer reflection nor to prolonged turbulence were obtained although enhanced E_s was observed. A bistatic phase-sounding network was deployed to the north of the explosion with ionospheric reflection points at 100-400-km ground ranges. The observed ionospheric disturbance corresponded to the passage of the acoustic wave at about 225 km altitude.

Acoustic waves from many other sources besides explosions have been detected in the ionosphere. Blanc (1982, 1984) described observations with a vertical incidence phase sounder following French underground nuclear tests. The disturbances resulted from the acoustic wave induced by the surface motion over the contained explosion. The ionospheric disturbance appeared as a

cyclical Doppler shift at F-region reflection heights and as a partial reflection at E-layer heights.

Ionospheric disturbances have also been observed after earthquakes and appear to be induced by acoustic waves launched by surface seismic waves traveling radially away from the epicenter. The disturbances have usually appeared as Doppler shifts in transmissions reflected in the F-region. Bistatic phase-sounding data collected after the Coalinga, California, earthquake showed changes in the spectra of the received transmissions that corresponded to the passage of the acoustic wave through the E-layer (Fitzgerald and Wolcott, 1985). These changes were interpreted as partial reflection signals from electron density gradients induced by the nonlinearly steepened acoustic wave. The partial reflections were Doppler shifted because the acoustic waves were propagating upward with the velocity of sound.

The Minor Scale explosion took place at 1820 UT (1220 MDT) on June 26, 1985. The bistatic phase-sounding experiment operated successfully and obtained data from -12 to +70 min. Ionospheric conditions created some problems for the experiment; there was intense E_s during most of the day. The E_s, combined with a low critical frequency for the F-region, made ionograms almost valueless. The bistatic frequencies therefore had to be chosen without a detailed knowledge of the ionospheric profile. In retrospect, it appears that the lowest frequency chosen (4.054 MHz) was reflected in the E-layer below the E_s. The two higher frequencies (4.854, 5.554 MHz) were reflected by the E_s-layer; because of the low F-critical, it would have been difficult to obtain F-propagation even if the ionospheric profile were known. All three frequencies showed disturbances after the explosion; the lowest frequency showed Doppler shifts indicative of the N-wave passing through the total reflection level and also showed some partial reflection. The two higher frequencies showed disturbances as the acoustic wave passed through the E-layer and also some disturbance corresponding in time to the acoustic wave passing through the F-region. We interpret the latter disturbance as a temporary F-mode created by the increase in the critical frequency induced by the passage of the acoustic wave.

II. EXPERIMENT

The receivers for the bistatic experiment were located at the Albuquerque Seismological Laboratory of the United States Geological Survey. The Laboratory is just off Kirtland Air Force Base at coordinates 34° 57′ N, 106° 22′ W and has an elevation of 1800 m. Power and communications were supplied by the Seismological Laboratory.

The transmitter station was located at the southern end of White Sands Missile Range at a ground range of about 140 km south of the explosion. Logistic support for the station at the Meteor Trail Radar Site was supplied by the Missile Range. The coordinates of the station were 32° 24′ N, 106° 30′ W; the elevation was about 1400 m.

Figure 1 shows the location of the transmitter and receiver stations in relation to the Minor Scale explosion. Ground zero was approximately 33° 38′ N, 106° 28′ W. The range between the transmitter and receiver was 283 km at an azimuth of 2.6° relative to true North. The midpoint between the receiver and transmitter stations was at 33° 40′ N, 106° 26′ W or 6.7 km from ground zero at an azimuth of 37°. Figure 1 also shows the locations of the Los Alamos vertical incidence phase sounder and HF radar and the French vertical incidence sounder.

Three Collins model HF-380 transmitters operating in unmodulated continuous wave (cw) mode were employed for the bistatic experiment. Such transmitters have been used in previous experiments including Mill Race. The output power was about 80 W. The frequencies of the transmitters appeared to show various levels of drift. This conclusion is based on the frequency of the signals observed at the receiver station and assumes that the receivers were stable. Such drifts have been observed previously and appear to be caused by temperature changes in the crystal ovens in the transmitters. A monitor receiver was not available at the transmitter station because all receivers were in use for the various experiments. The drifts ranged from 0.05 to 0.2 Hz/min and appear to be constant in time over periods of 15 min.

Separate receivers, Racal model RA6790 GM, were used for each transmitter frequency. The receivers were operated in cw mode at a beat frequency of about 50 Hz and without automatic gain control. Manual gain control reduces the occurrence of artificial harmonic signals generated by the receiver. These receivers have been used on previous experiments and have proved reliable and stable in frequency.
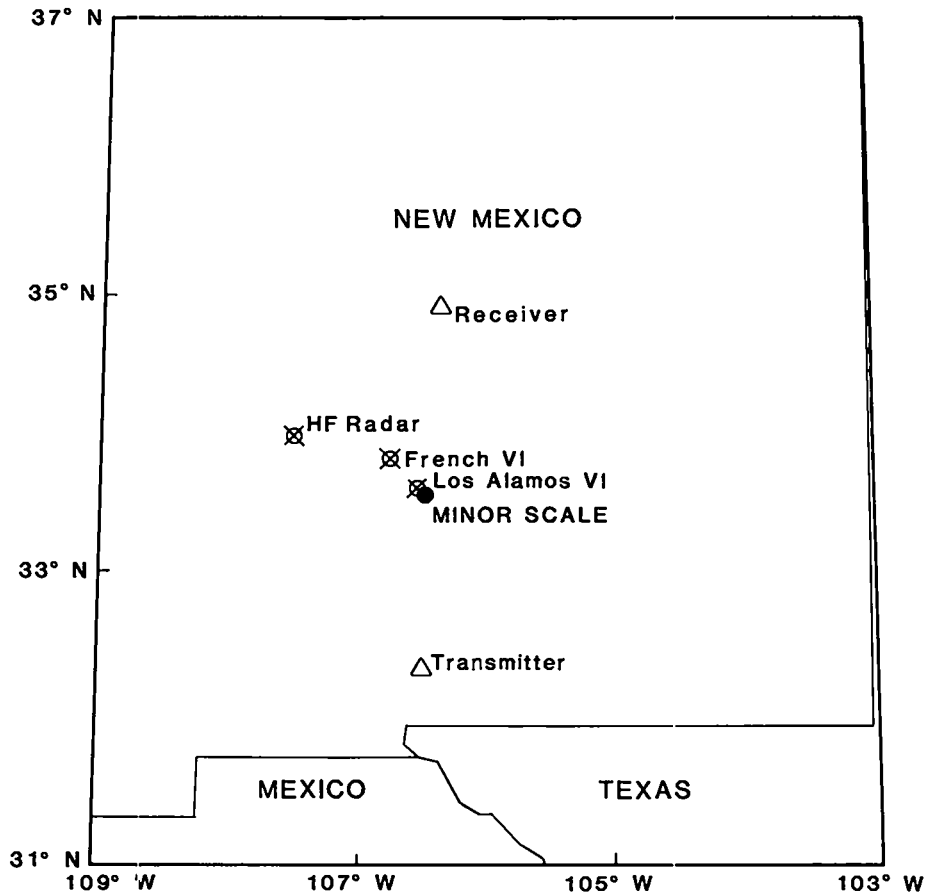
6

Fig. 1. Location of the transmitting and receiving stations for the bistatic experiment in relation to the Minor Scale explosion and the vertical incidence sounders.

The bandwidths of the receivers were controlled by built-in lowpass filters and were set to the minimum possible values; for two of the receivers this value was 100 Hz, while for the other (5.554 MHz) it was 1.2 kHz. An audio spectrum analyzer was used at the output of the receivers to monitor signal strength and interfering signals in the bandpass of the receivers.

French-designed, tilted V-antennas were used for both receiving and transmitting. The V had legs 36 m long, and the apex of the V was raised to a height of 10 m with an aluminum mast. The open end of the V was at ground level; each tip of the V was terminated with a 200-Ω resistor to a ground plane wire that ran back to the mast. The antennas were designed to have a high gain directed toward the open end of the V. Because of the unequal loading, winds bent some of the masts, which made operating the antennas difficult. One antenna was used at the receiver station; the signal was split two times to

feed the three receivers. At the transmitter station a separate antenna was used for each transmitter. Although the antennas did not overlap, they were closely enough spaced that some mutual coupling probably affected their radiation patterns.

A four-channel audio tape recorder, Tascam model 34, was used to record the output of the receivers. Magnetic tape 1/4 in. wide on 10-in. reels was used, and each receiver output was placed on a separate track. The recording speed was 19 cm/s; the recording system has a 30-Hz to 20-kHz bandwidth. This recording technique has been used on previous experiments also. The fourth track of the tape recorder was used for a 1-kHz IRIG-B time code derived from a receiver for a Geostationary Orbit Environmental Satellite (GOES) beacon; the receiver was directed to the east satellite.

To conduct a detailed analysis of the received signals, the audio tape recording was digitized after the experiment. The sampling rate was 250 Hz for each track; the sampling interval was derived from the 1-kHz time code in order to mitigate the effects of tape speed variation. The replay output of the tape recorder was lowpass filtered (bandwidth about 100 Hz) before being digitized. This effectively equalized the bandwidths of the different tracks and reduced aliasing of the spectrum.

It became clear during the days preceding the Minor Scale explosion that the ionosphere was not going to cooperate fully with our desires for propagation conditions. Intense E_s was observed during most of the daytime; the critical frequency of the F-layer was unusually low. Such conditions may be ascribed to the time of year and to the minimum in the current solar cycle (sunspot number of 10). Bistatic propagation was obtained over a frequency range of 3.5 to 12 MHz on the day of the explosion. Similar conditions prevailed on previous days. The greatest signal strength, 40 dB above background, was obtained at 8 MHz; at 5 MHz the signal level was about 20 dB. Interestingly, the signal strength improved to 30 dB at 4 MHz.

Both the ionograms and the extended frequency range of the bistatic propagation showed clearly that there was intense E_s at the time of the Minor Scale explosion. We assume that propagation above 5 MHz was by reflection from the E_s-layer. The increase in signal strength at 4 MHz may have been due to better propagation from the normal E-layer in comparison with the E_s-layer.

Because of the E_s, ionograms obtained with the HF radar and virtual heights obtained with the vertical incidence phase sounder were spotty and difficult to interpret. Based on ionograms obtained before the event and on educated guesswork, we believe that the critical frequency of the E-layer was between 3.2 and 3.5 MHz; the ionograms appear to show an Fl-layer with a critical frequency between 4.0 and 4.5 MHz. The vertical incidence phase sounder detected a very high F-region return (600-km virtual height) at a frequency of 4.2 MHz during some periods within an hour after the explosion. This intermittent echo would indicate a critical frequency close to 4.2 MHz for the F-layer.

Under the perverse ionospheric conditions that prevailed in the hours leading up to the explosion, we decided to limit the frequencies to the 4.0-5.5-MHz range in order to obtain E- and F-propagation if possible. Although the signal was stronger at higher frequencies, the propagation was clearly not F-region; if a fourth transmitter-receiver system had been available, it would have been placed at about 7 MHz. The frequencies finally selected were 4.054, 4.854, and 5.554 MHz.

Because no complete ionogram was obtained near the explosion, the electron density profile remains unknown and no ray traces have been attempted. E- and E_s-reflections are almost specular, so the ionospheric reflection points correspond to the midpoints of the paths.

III. RESULTS

Our analysis methods are relatively standard; in order to obtain a time history of the spectra of the received signals, we use the overlapped Fourier transform method. For example, we calculate the power spectrum of 10 s of data, then advance 2 s and calculate a new spectrum from 10 s of data so that there is an 80% overlap of data. We apply a Kaiser-Bessel window to the data before taking the fast Fourier transform in order to reduce spectral leakage. This method gives some smoothing in time while permitting adequate spectral resolution; it also allows us to follow spectral changes over an extended period of time.

To present the spectral time histories we use a three-dimensional display in which we show power at a given frequency for successive time periods. We use a color code to indicate relative power level; the code is indicated on a color scale accompanying the spectral history. The frequency interval is

9

0.1 Hz, which is the inverse of the data window. Figure 2 shows the time history of the spectrum of the 4.054 MHz between 0 and 960 s after the explosion. The main signal peak was at 49.5-Hz frequency and showed a -0.03-Hz/min frequency drift. This frequency had a relatively good signal-to-noise ratio; it also appears that the signal level was more stable for this frequency than for the other two frequencies.

A distinct shift in the frequency of the main signal peak occurred about 305 s after the explosion; initially the shift was about -1 Hz, but it decreased in magnitude with time and returned to 0 at 325 s. A slight positive excursion preceded the abrupt -1-Hz shift and also preceded the end of the episode of disturbance.

Figure 2 shows a peak at approximately -3-Hz relative Doppler that appeared at 300 s and rapidly merged with the main signal peak, which had shifted by -1 Hz. A similar but weaker peak occurred at 320 s but appeared to fade without merging with the main signal peak. It should be noted that some spectral smearing is inevitable in these data because of the frequency shifts within the analysis time window.

As can be seen in Fig. 2, the abrupt frequency shift of the main peak coincided with an equally abrupt increase in signal level of about 10 dB. This increase can also be seen in Fig. 3, where we have plotted the total signal level versus time for the 4.054-MHz transmission between 250 and 350 s after the explosion. The abrupt increase in power occurred at 305 s. Close inspection of the spectra in Fig. 2 shows that the signal level of the main peak faded by about 5 to 10 dB just before the negative Doppler shift. The signal level decreased steadily as the Doppler shift decreased and faded by about 5 dB just before the Doppler returned to zero.

The frequency of the main signal showed short period variations until about 400 s after the explosion. The width of the spectral peak remained broadened at the -30-dB level until about 700 s.

The time history of the 4.854-MHz transmission between 0 and 960 s after the explosion is shown in Fig. 4. The major component of the spectrum was initially at 47 Hz but showed a -0.15-Hz/min frequency drift. This link had the lowest signal-to-noise ratio of the three. A broad peak at about -5 Hz relative to the main peak appeared at 380 s after the explosion. The signal level of this peak was about -10 dB relative to the main peak. This peak persisted for at least 460 s, after which it appeared to drift toward the main
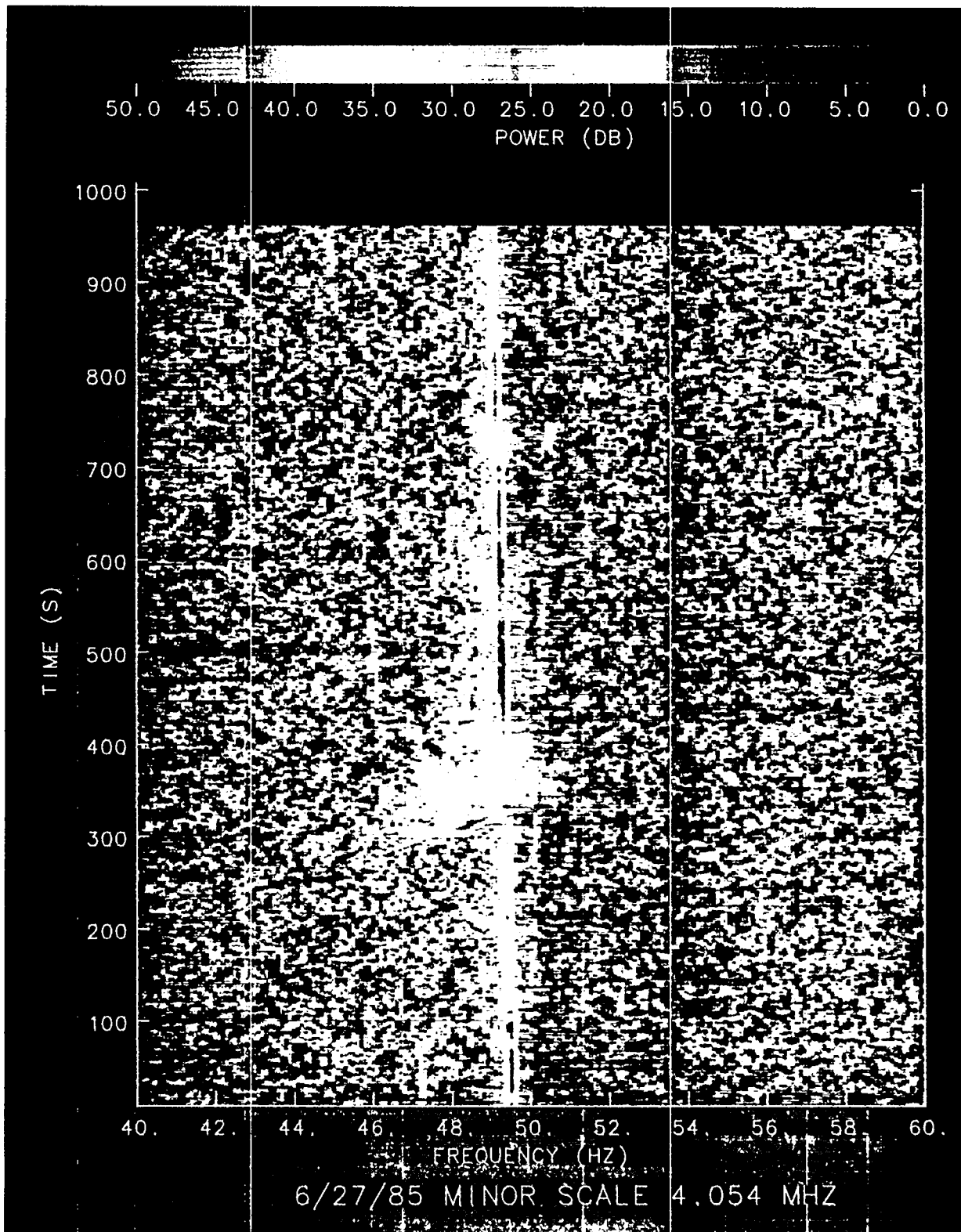
Fig. 2. Time history of the spectrum of the 4.054-MHz link. Power at a given frequency is coded according to the color scale at the top. The abscissa is frequency in Hertz referenced to an arbitrary zero frequency. The ordinate is time in seconds after the explosion. A disturbance occurs between 300 and 350 s.
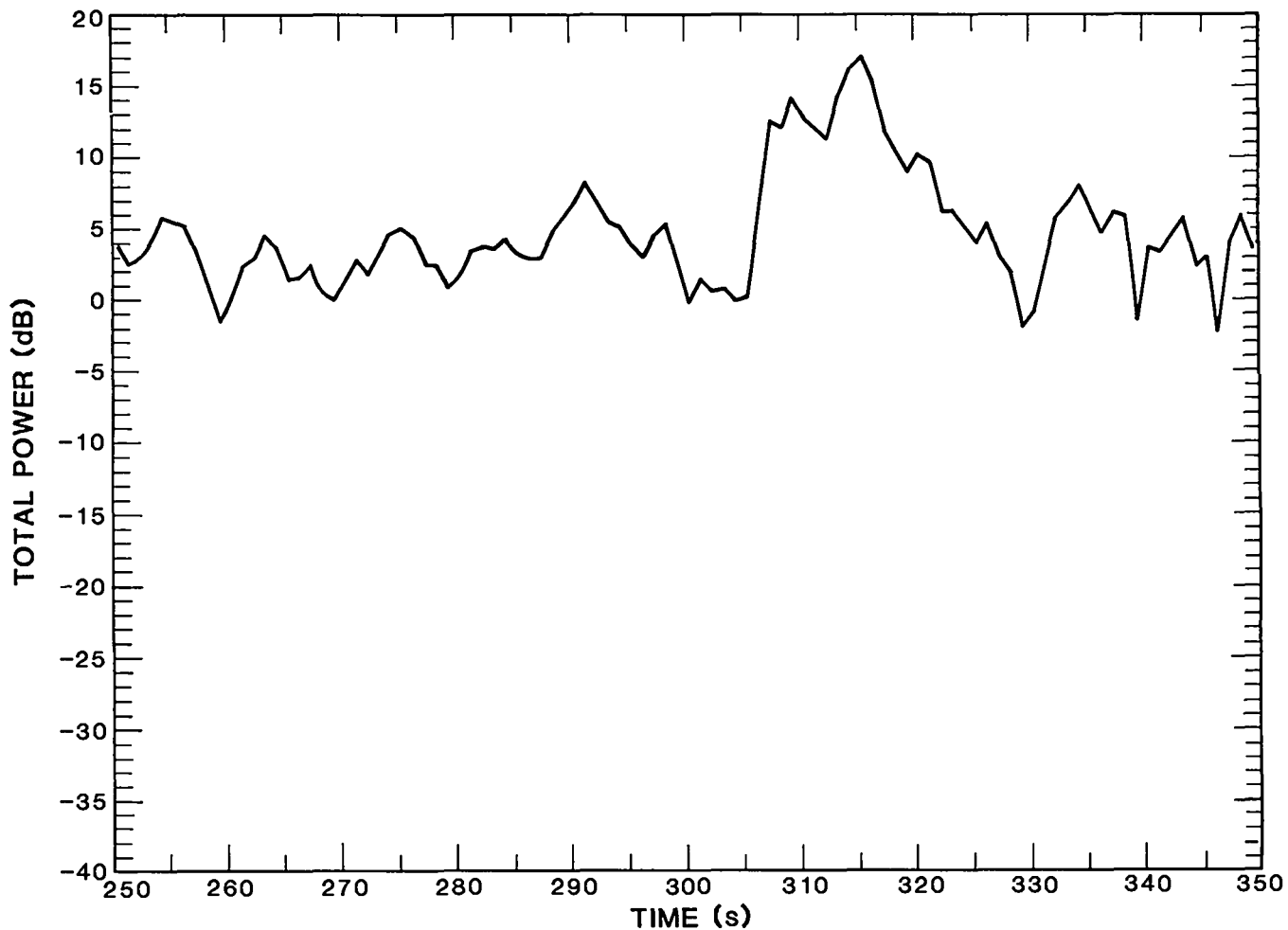
Fig. 3. Total received power for the 4.054-MHz link between 250 and 350 s after the explosion. There is an enhancement of 15 dB at 305 s.

peak before finally disappearing at about 550 s. We also note in Fig. 4 the appearance of two peaks at the -20-dB level at about -10-Hz relative Doppler between 450 and 500 s. They appear to progress with time toward more 'negative Doppler shifts.

At least two peaks appear in Fig. 4 at negative relative Doppler 300 to 350 s after the explosion. They progress with time toward lower Doppler shifts. The spectrum was very much disturbed during that period and showed a number of peaks at negative Doppler.

The frequency of the main peak showed disturbances of a few tenths of a hertz for a few minutes after the disturbances recorded between 300 and 350 s. The spectrum remained broadened at the -30-dB level until 700 or 800 s after the explosion. We note that there was no distinct Doppler shift in the main signal peak at this frequency as was found in the data obtained at 4.054 MHz.
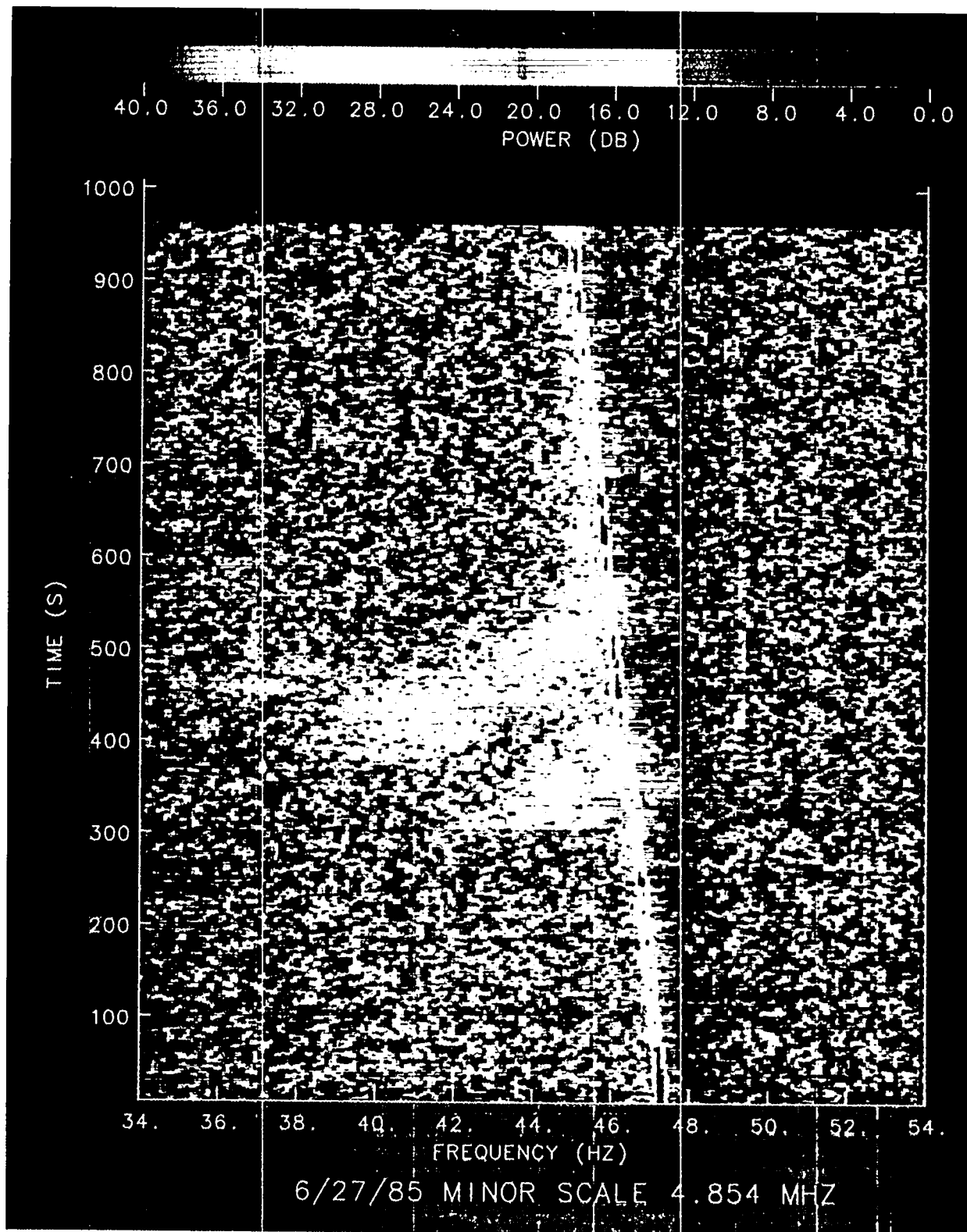
12

Fig. 4. Time history of the spectrum of the 4.854-MHz link. The display is the same type as that shown in Fig. 2. A disturbance consisting of peaks with rapidly changing frequency occurs between 300 to 350 s. A broad peak centered at 42 Hz occurs 380 to 480 s after the explosion.

Figure 5 displays the time history of the spectrum of the 5.554-MHz transmission between 0 and 960 s after the explosion; the only prominent line component is at 50 Hz, which shows a +0.03-Hz/min frequency drift. The signal strength was relatively good on this link.

A broad peak appears in the spectrum 380 to 460 s after the explosion at a frequency of -7 Hz relative to that of the main peak. The power level of the peak was about -20 dB relative to that of the main peak. A strong peak appeared at negative Doppler shift after 300 s; the frequency offset rapidly decreased with time and then appeared to continue for a few seconds at positive Doppler.

The frequency of the main peak showed tenth hertz variations for a minute or so after the negative Doppler peak appeared at around 300 s. The width of the main spectral peak at low power levels remained broadened for a few minutes after 300 s. No Doppler shift in the main signal peak appeared at this frequency in contrast to the data at 4.054 MHz.

IV. INTERPRETATION

For this report, we have chosen to concentrate on three prominent features in the bistatic data obtained during the Minor Scale experiment. These features are (1) the Doppler shift episode and the accompanying change in signal strength at 300 s observed in the 4.054-MHz transmission; (2) the peaks at negative Doppler, which also occurred during this episode; and (3) the broad peaks at -5 and -7 Hz, which occurred between 380 and 460 s in the higher frequency transmissions.

In the absence of a good ionogram we have conjectured a likely electron density profile to interpret some of the results of our experiment. We assume that the ionosphere, ignoring the E_s, was made up of two parabolic layers. One with a 3.2-MHz critical frequency and a 10-km width and centered at 100 km altitude represented the normal E-layer. The other with a 4.2-MHz critical frequency and a 50-km width and centered at 190 km altitude represented the F-layer. Using the analytical result for the virtual height of parabolic layer when the ambient magnetic field is zero, we can obtain the conjectural ionogram shown in Fig. 6. Of course, we have oversimplified the true F-region profile, which probably contained equally strong F1- and F2-layers.
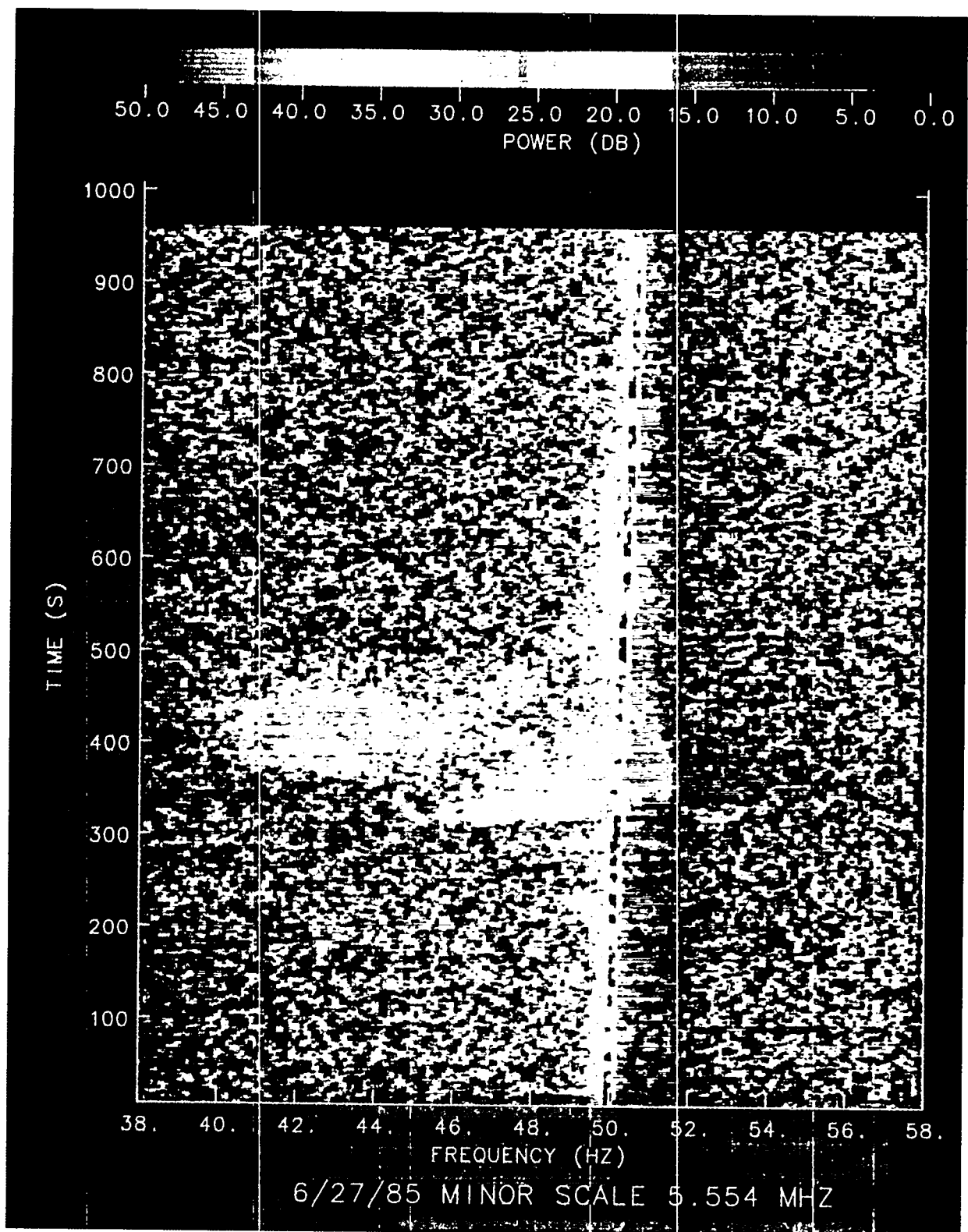
Fig. 5. Time history of the spectrum of the 5.554-MHz link. The display is the same type as that shown in Fig. 2. A broad peak centered at 43 Hz occurs 380 to 480 s after the explosion.
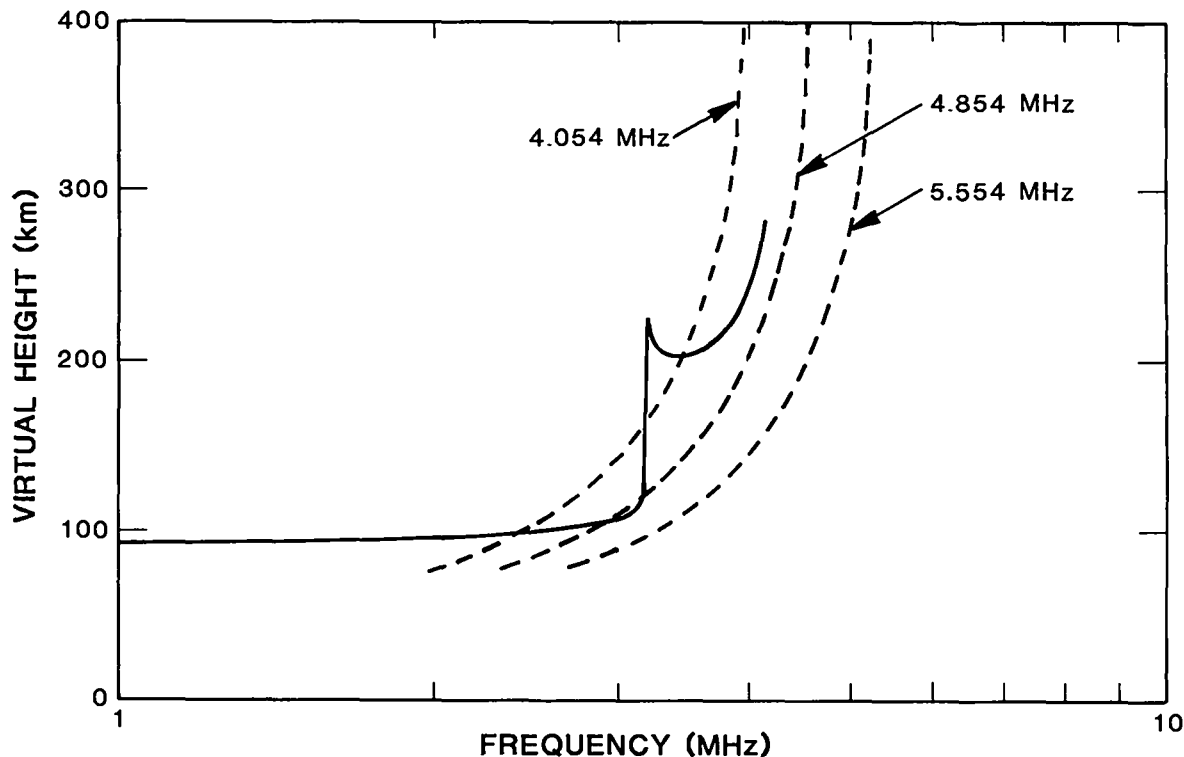
15

Fig. 6. Ionogram constructed by assuming two parabolic layers: one at 100-km altitude, 10-km width, and 3.2-MHz critical frequency and the other at 190-km altitude, 50-km width, and 4.2-MHz critical frequency. The other curves represent the equivalent vertical frequencies versus group height for the three bistatic transmissions.

We can obtain the expected ray paths for this ionosphere by plotting the effective vertical frequency versus virtual height for the distance between receivers and transmitters (Davies, 1969). These curves for the three frequencies are shown in Fig. 6. The curve for the 4.054-MHz transmission intersects the ionogram at the normal E-layer and possibly at a higher level. The most likely propagation mode would be reflection from the normal E-layer at an equivalent vertical frequency of 2.5 MHz. On the other hand, the curve for the 5.554-MHz transmission never intersects the ionogram, indicating that neither normal E-layer nor F-propagation was possible. The curve for the 4.854-MHz transmission just grazes the ionogram at the E-layer but not at any other level; the E-layer mode would be just at the edge of the skip zone. For the assumed model ionosphere, no F-region propagation would be expected at either of the two higher frequencies.

The E_s was almost blanketing up to 4 MHz (vertical); the likely propagation modes of the 4.854- and 5.554-MHz oblique transmissions were therefore by reflection from this layer. The relatively stable frequency of these transmissions (ignoring the linear drift) also indicates that these were not F-modes. It is likely that the 4.054-MHz transmission was reflected in the normal E-layer at an altitude below that of the E_s.

We believe that the Doppler shift and the change in signal level, which occurred after 300 s on the 4.054-MHz data, were caused by an acoustic wave with N-shaped profile propagating through the total reflection level in the E-layer at approximately 95 km altitude. We have attempted to model the Doppler shift and reflection coefficient that such a wave would produce. To do this we employ the phase integral method (Budden, 1961) in which the reflection coefficient is given by

$$R = i \exp \left(-2ik \int_o^{z_o} q(z)dz \right) , \tag{2}$$

where q is a root of the Booker quartic and the integral is over a path from the ground to the reflection height, z_o, where $q(z_o) = 0$. The reflection point, z_o, is complex. For oblique propagation at frequency f when there is no ambient magnetic field, q is given by

$$q^2 = \cos^2 I - \frac{f_N^2/f^2}{1 - iZ} , \tag{3}$$

where $\cos I$ is the cosine of the angle of incidence on the ionosphere, Z is the ratio of the collision frequency to the radian wave frequency, and f_N is the plasma frequency. As is well known, the phase of R can be calculated by inserting the equivalent vertical frequency, $f_v = f \cos I$, which reduces the problem to vertical propagation at frequency f_v (Davies, 1969). The absorption can also be calculated as if for vertical propagation at f_v, but the coefficient must be multiplied by $\cos I$ to obtain the correct value (Davies, 1969). We assume a Chapman layer for the background electron density, so the plasma frequency, $f_N(h)$, is given by

$$f_N^2 = f_o^2 \exp \left(1 - (\frac{h-h_o}{H}) - \exp (\frac{h-h_o}{H}) \right) \qquad (4)$$

with a maximum, f_o, of 3.2 MHz at altitude $h_o = 105$ km and with a scale height $H = 10$ km. The collision frequency, $\nu(h)$, is assumed to be exponential with a value of 3.65×10^4 at 100 km and a scale height of -7 km. The N-wave profile is assumed to have a constant amplitude, D, and length, l_o, of 7000 m at h_o and is given by

$$p(h-h_o-v_o t) = \begin{cases} 2D(h-h_o-v_o t)/(l_o + 2D\,v_o t) & |h-h_o-v_o t| \leqslant \dfrac{l_o}{2} + Dv_o t \\[2em] 0 & \text{otherwise} \end{cases} \qquad , \quad (5)$$

where v_o, the sound speed, is assumed constant at 300 m/s. We assume in Eq. (5) that the length of the profile increases with time because of the nonlinear stretching that accompanies acoustic propagation. The amplitude of the profile is constant.

If $N_o(h)$ is the ambient electron density, then the equation of continuity gives

$$\frac{\partial N'}{\partial t} + \nabla \cdot (N_o \bar{V}) = 0 \quad , \qquad (6)$$

where $N'(h,t)$ is the electron density perturbation (Yeh and Liu, p. 420). Equation (6) may be solved for N' to give

$$N'(h,t) = N_o\, p(h-h_o-v_o t) + \frac{\partial N_o}{\partial h} \int_{-\infty}^{h-h_o-v_o t} P(\zeta)d\zeta \quad . \qquad (7)$$
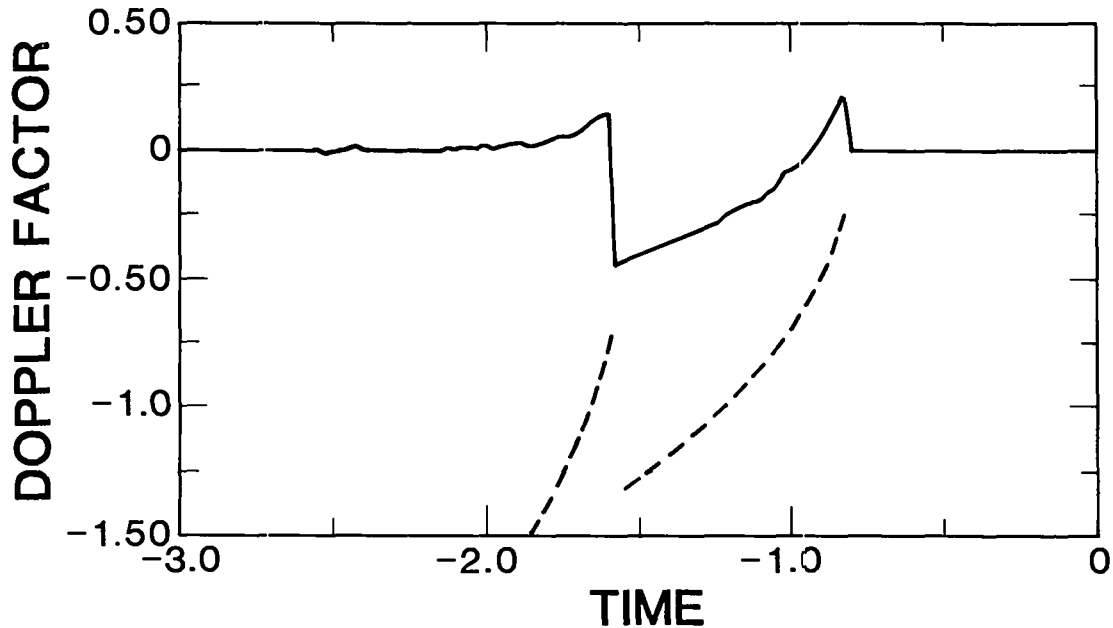
18

Fig. 7. Calculated Doppler shift produced at an equivalent frequency of 2.50 MHz by an N-wave of relative overdensity 15% (solid curve). A Chapman layer with a 3.2-MHz critical frequency is assumed for the background electron density. The dashed curves show the Doppler shift of partial reflections from the leading and trailing edges of the N-wave. Time units are estimated to be 23 s; Doppler units to be 2.5 Hz.

The second term on the right-hand side of Eq. (7) becomes important when the dimensions of the perturbation are comparable to the ambient electron density scale height. This condition is true in the E-region for our model.

Figure 7 shows the calculated Doppler shift, which is the negative derivative of the phase of the reflection coefficient versus time. The units on the graph are dimensionless; the actual time may be obtained by multiplying the units by the length, l_0, of the acoustic wave at h_0 divided by the velocity of sound, v_0, or roughly 23 s. The Doppler is in units of v_0/c times the effective vertical frequency of the transmitted wave or about 2.5 Hz. The Doppler shift is initially positive, then abruptly goes negative when the reflection height changes; it gradually shifts to positive values before returning to the undisturbed level. In order to obtain a Doppler shift of the proper magnitude, we have to assume an overdensity of 15% if the sound speed is taken as 300 m/s and the vertical frequency as 2.5 MHz. The calculated Doppler shift in these dimensionless units is independent of the length of the acoustic wave.
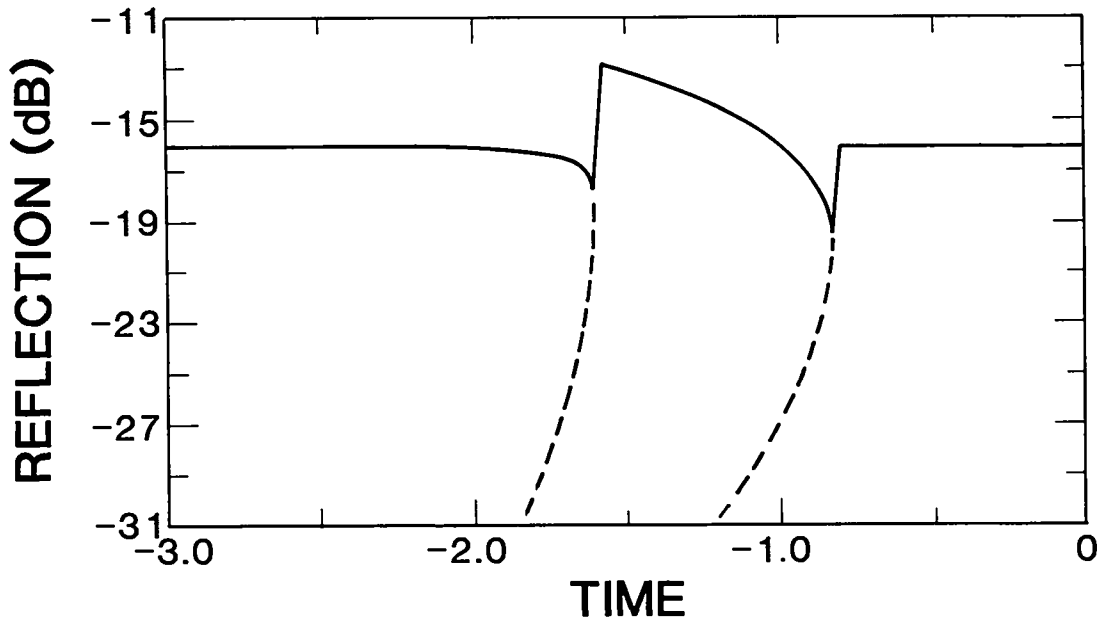
19

Fig. 8. Calculated reflection coefficient of a 2.5-MHz equivalent vertical frequency versus time for an N-wave incident upon a background Chapman layer with an exponentially decreasing electron-neutral collision frequency. The dashed curves represent the power partially reflected from the leading and trailing edges of the N-wave.

The reflected power versus time is shown in Fig. 8; this calculation depends critically upon the assumptions about the collision frequency and the absolute reflection height and also on the length units. The calculation does show an initial fade, then an abrupt increase in signal power followed by a slower fade before returning to the undisturbed level. The increase in signal power results from the abrupt lowering of the reflection height when the plasma frequency in the overpressure portion of the N-wave reaches the equivalent vertical frequency of the HF wave. The decrease in path length leads to a decrease in absorption. As stated by Davies, the absorption change mirrors the group height change for a vertically incident wave.

The leading and trailing edges of the N-wave have widths on the order of the mean free path, which in the E-region of the ionosphere is less than a few meters; because the wavelength of the HF wave is about 100 m, partial reflections from the edges of the N-wave are possible (Blanc, 1982; Fitzgerald and Wolcott, 1985). These partial reflections will be Doppler-shifted from the frequency of the total reflection because of the upward motion of the N-wave. The Doppler shift and the reflection coefficient will vary in time because the

index of refraction at the reflecting layer is constantly varying. We have attempted to model the Doppler shift and reflected power in order to interpret the other peaks in the spectrum of the 4.054-MHz data. The calculation can be carried out as if for vertical propagation at the equivalent frequency if we ignore the ambient magnetic field. We have further simplified the calculation by assuming that the equivalent frequency is constant, thereby ignoring changes in group height induced by the N-wave.

We have calculated the Doppler shift for the partial reflections in a manner similar to the calculation for the total reflection except that the phase path is integrated only up to the leading or trailing edge. The results are shown in Fig. 7. Initially, the Doppler is relatively high because the index of refraction is close to unity; consequently, the phase path change is close to the actual path change. As the reflecting edge approaches the total reflection level, the index of refraction and therefore the Doppler decrease rapidly. The Doppler shifts of the total reflection and the partial reflections merge at the transition times when the overpressure in the N-wave causes the abrupt decrease in reflection height and again when the underpressure of the N-wave reaches the total reflection height and abruptly ends the disturbance.

We calculated the power for the partial reflections by assuming that it was controlled by two effects: the index of refraction change at the edge and the absorption along the ray path. We assume that the boundary is infinitely sharp so that the partial reflection coefficient is given by the Fresnel formula at vertical incidence

$$R = \frac{\mu_1 - \mu_2}{\mu_1 + \mu_2} , \tag{8}$$

where μ_1 and μ_2 are the indices of refraction on either side of the transition. The absorption and the total reflection are both found by integrating the imaginary part of the refractive index up to the reflecting surface. The results for the calculation are shown in Fig. 8. The reflected power from the leading and trailing edges does not show the same time history because the reflection heights and therefore the absorption are different. For the upper edge, the partial reflection power increases rapidly to become greater than

21

that of the total reflection just before the power of the total reflection abruptly increases. Comparing the Doppler shift calculation, Fig. 7, with the reflected power calculation, we see that the partial reflection from the upper edge merges into the total reflection. On the other hand, the partial reflection power from the lower edge eventually becomes greater than the total reflection power near the end of the disturbance, but the partial power never becomes greater than the quiescent reflected power.

In the absence of a good ionogram it is difficult to interpret the data at 4.854 and 5.554 MHz; we assume that the overpressure of the acoustic wave in the F-region increased the critical frequency enough to make possible temporary F-modes. Because the acoustic wave was moving upward, the reflection, total not partial, would have a high Doppler. This is a possible explanation for the peaks at negative Doppler seen between 380 and 480 s.

To obtain bistatic propagation at 4.854 MHz, the critical frequency of the F-region would have to be increased to about 4.4 MHz, which corresponds to an overdensity of 10%. To achieve propagation at 5.554 MHz (0-mode), the overdensity would have to be at least 40%. A more likely alternative is that the peak in the 5.554-MHz spectra arose from X-mode propagation. For transverse propagation, an X-mode corresponds to an 0-mode at 0.5- to 0.7-MHz lower frequency. That is, X-mode propagation at 5.554 MHz would roughly correspond to 0-mode propagation at 4.854 MHz.

We might expect the X-mode at 4.854 MHz to be totally reflected in the F-region. Why do we see no disturbance corresponding to this total reflection? There is a considerable difference in absorption between 0- and X-modes; at 4.854 MHz the X-mode is estimated to be 30 dB less than the 0-mode for our conditions. The difference in signal level would make it difficult to observe an X-mode disturbance. Moreover, we observed no F-region disturbances at 4.054 MHz, which would be the approximate equivalent frequency of the X-mode at 4.854 MHz. It is therefore possible that the 4.854-MHz X-mode did not propagate in the F-region. We would not expect to see E-layer disturbances for the X-mode because it would be highly absorbed at that altitude.

We have calculated the Doppler to be expected from a temporary F-region propagation mode; we assumed that the background ionosphere was a parabolic layer with a critical frequency 0.95 that of the transmission frequency. The width of the parabolic layer was assumed to be 6 times the width of the acoustic wave profile. The density perturbation has the profile shown in

Fig. 9; the acoustic wave is no longer a sharp N-wave but now has rounded edges. The maximum amplitude is 13%. The resulting Doppler is shown in Fig. 10; we see a temporary mode with a Doppler of about -0.6 to -0.7. If the profile width was approximately 25 km and the sound speed was 500 m/s, the time unit is about 50 s. For a sound speed of 500 m/s and an equivalent vertical frequency of 4.2 MHz, the units of Doppler frequency are 7 Hz. For the 5.554-MHz X-mode, the equivalent vertical frequency would be 4.8 MHz and the Doppler units 8 Hz. The predicted Doppler during the period shown in Fig. 10 when it is almost constant is about -0.65 which corresponds to -4.5 Hz for the 4.854-MHz path and -5.0 Hz for the 5.554-MHz path.

Of course, the acoustic profile changes during its vertical propagation, an effect that our model neglects. We also ignore the changes in effective vertical frequency as the reflection height and therefore the virtual height increase with time. Our model does not touch upon the width of the spectral peaks, which may have arisen from multiple reflections with varying Doppler shift.

V.   CONCLUSIONS

Our model calculations show good agreement with the 4.054-MHz data and support our conclusion that we observed an N-wave from the Minor Scale explosion passing through the total reflection height in the E-layer. We base this conclusion on the form of the Doppler shift in the total reflection, the change in absorption for the total reflection, the Doppler shift for the partial reflection, and the partial reflection power. We estimate that at the E-layer the N-wave had an overdensity of approximately 15% and a length of 7 km.

Our model calculations also support the conclusion that the acoustic wave temporarily raised the critical frequency in the F-region enough to support bistatic propagation at 4.854 and 5.554 MHz. The overdensity in this region may have been as great as 13%.

The data obtained by the Los Alamos vertical sounder, located close to the explosion, appeared to show no total reflection in the E-layer in the four frequencies between 3.2 and 4.2 MHz. This result appears to indicate that the critical frequency was less than 3.2 MHz. During the 300- to 350-s time period, all four frequencies showed disturbances similar to those appearing on the two higher frequencies in the bistatic data at the same time. We have not
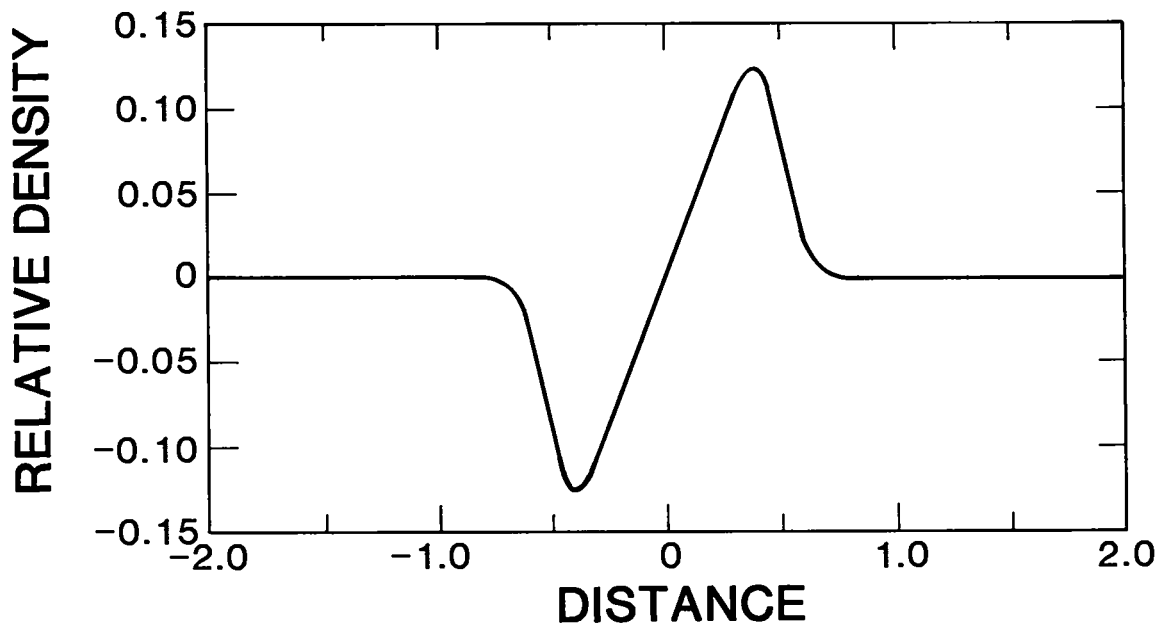
Fig. 9. Acoustic wave profile assumed for F-region calculation. The overdensity is 13%. Distance units are approximately 25 km.
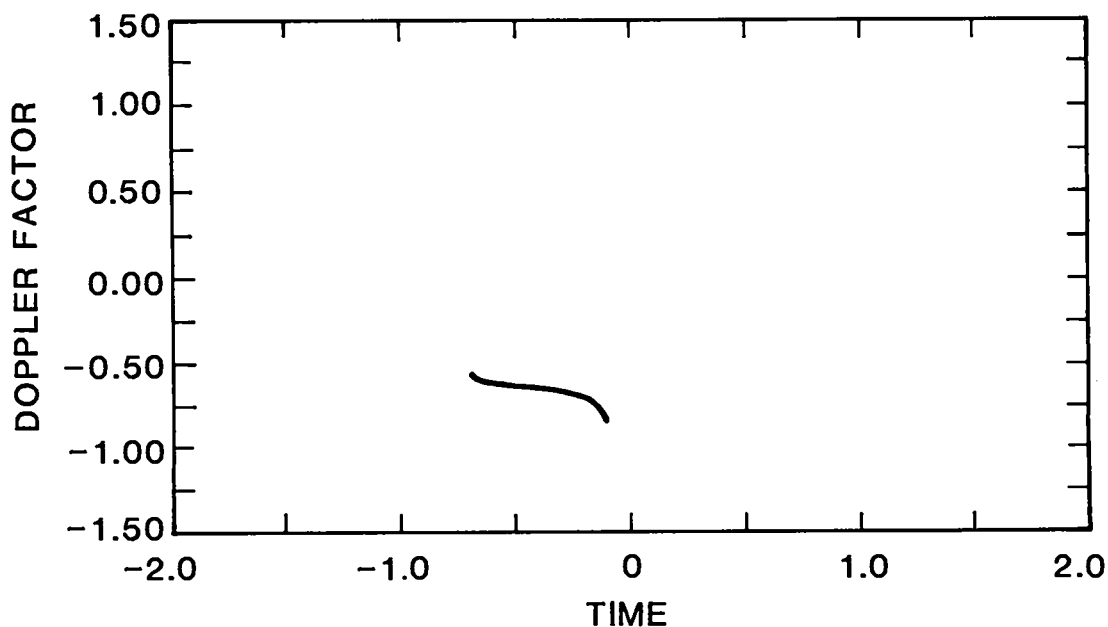

Fig. 10. Predicted Doppler shift versus time for a 4.4-MHz equivalent vertical frequency incident upon an ionosphere made up of a parabolic layer with a 4.2-MHz critical frequency when the acoustic wave with profile shown in Fig. 9 propagates upward at a speed of 500 m/s. The units of time are roughly 50 s; those of Doppler are 7 Hz.

looked at those disturbances in detail for this report. The 4.2-MHz vertical sounding data show a peak at negative Doppler between 420 and 540 s after the explosion that appears to be related to the F-region peaks appearing in the bistatic data described above. The peaks appear initially at a group height of about 150 km and move upward with time. These data appear to be in agreement with the supposition that the overpressure raised the F-critical-frequency in a layer that moved upward in time and produced a temporary path with a high negative Doppler shift. A full discussion of these results will appear in a future report.

The ionograms obtained during the Buster-Jangle explosions enabled Kanellekos and Nelson (1972) to follow the leading and trailing edges of the acoustic wave up to 200 km altitude. They did not obtain results on the overpressure from these ionograms. Our data do not allow us to follow the whole acoustic wave through the F-region; however, such data might shed some light on one aspect of the Buster-Jangle ionograms. Between 5 and 6 min after the explosions, the ionograms showed two-hop E-layer propagation when none had previously been showing. This occurrence appears to correlate with the passage of the acoustic wave through the E-layer. From our analysis we would expect an increase in the reflection coefficient from the E-layer during this period, so two-hop propagation might suddenly appear and then disappear as the acoustic wave advances into the F-region.

The bistatic experiment described in this report has yielded useful results on the ionospheric disturbance produced by a large explosion. This is especially true for the disturbance in the E-layer. If similar experiments are contemplated in the future, it would be useful to obtain group path information, for example, with a $d\phi/d\omega$ technique (Baulch et al., 1984). A 100- to 150-km ground path between transmitter and receiver would also enable easier sounding in the F-region. It appears that the major difficulty in the experiment, the ionospheric conditions, cannot be controlled.

and kept us informed of the status of the test. Hal deHaven assembled the equipment necessary for the experiment, and Bob Carlos digitized the resulting data. Jim Walker and Rubel Martinez ably manned the transmitting station.

REFERENCES

Barry, G. H., L. J. Griffiths, and J. C. Taenzer, "HF radio measurements of high-altitude acoustic waves from a ground level explosion," J. Geophys. Res., 71, 4173 (1966).

Baulch, R. N. E., E. C. Butcher, J. C. Devlin, and P. R. Hammer, "A simple sounder to measure the properties of ionospherically reflected radio waves," J. Atmos. Terr. Physics, 46, 895 (1984).

Blanc, E., "Neutral temperature and electron-density measurements in the lower E region by vertical HF sounding in the presence of an acoustic wave," Geophys. Res. Lett., 9, 450 (1982).

Blanc, E., "Interaction of an acoustic wave of artificial origin with the ionosphere as observed by vertical HF sounding at total reflection levels," Radio Science, 19, 653 (1984).

Budden, K. G., Radio Waves in the Ionosphere (Cambridge University Press, Cambridge, 1961).

Davies, K., Ionospheric Radio Waves (Blaisdell, Waltham, Massachusetts, 1969).

Fitzgerald, T. J., and J. H. Wolcott, "E-layer ionospheric disturbances following the Coalinga earthquake," Los Alamos National Laboratory report LA-10607-MS (1985).

Jacobson, A. R., R. C. Carlos, P. E. Argo, and D. G. Rickel, "Radio-wave diffraction during the passage of an acoustic shock through a sporadic-E layer," submitted to Radio Science (1986).

Kanellakos, D. P., and R. A. Nelson, "Comparison of computed and observed shock behavior from multikiloton, near-surface nuclear explosions," in Effects of Atmospheric Acoustic Gravity Waves on Electromagnetic Wave Propagation, AGARD-CP-115, NATO (1972).

Rickel, D. G., and D. J. Simons, "The acoustic at ionospheric heights caused by the Mill Race explosion," Los Alamos National Laboratory document LA-UR-82-618.

Yeh, K. C., and C. H. Liu, Theory of Ionospheric Waves (Academic Press, New York, 1972).

Page Range	NTIS Price Code		Page Range	NTIS Price Code		Page Range	NTIS Price Code		Page Range	NTIS Price Code
001-025	A02		151-175	A08		301-325	A14		451-475	A20
026-050	A03		176-200	A09		326-350	A15		476-500	A21
051-075	A04		201-225	A10		351-375	A16		501-525	A22
076-100	A05		226-250	A11		376-400	A17		526-550	A23
101-125	A06		251-275	A12		401-425	A18		551-575	A24
126-150	A07		276-300	A13		426-450	A19		576-600	A25
									601-up*	A99

*Contact NTIS for a price quote.

Los Alamos